



Investigation on shape transferability in ultraprecision glass molding press for microgrooves

Tianfeng Zhou^a, Jiwang Yan^{a,*}, Jun Masuda^b, Takashi Oowada^a, Tsunemoto Kuriyagawa^a

^a Department of Nanomechanics, Graduate School of Engineering, Tohoku University, Aoba 6-6-01, Aramaki, Aoba-ku, Sendai 980-8579, Japan

^b Toshiba Machine Co., Ltd., 2068-3, Ooka, Numazu-shi, Shizuoka-ken 410-8510, Japan

ARTICLE INFO

Article history:

Received 12 February 2010

Received in revised form 30 June 2010

Accepted 20 July 2010

Available online 19 September 2010

Keywords:

Glass molding press

Microforming

Microgroove

Finite element method

Shape transferability

ABSTRACT

Glass molding press (GMP) has been applied to produce the microgrooves on glass plates by using electroless-plated nickel phosphorus (Ni–P) molds. The GMP process for microgrooves was analyzed by finite element method (FEM) simulation. The effects of various pressing conditions, such as the molding temperature, the pressing velocity and the friction in glass deformation, were studied. Then, based on the simulation results, optimal pressing conditions were determined and used in the GMP experiments. By comparing the shape of the molded microgrooves with that of the corresponding microgrooves on the Ni–P mold, the shape transferability was evaluated and the reasons for form error were analyzed. The results show that the GMP process is an effective way to fabricate precision microgrooves on glass.

© 2010 Elsevier Inc. All rights reserved.

1. Introduction

Three-dimensional microsurface structures such as microgrooves, micropyramids, microprisms and microlenses are required more and more in recent optical, optoelectronic, mechanical and biomedical industries [1]. Components with microsurface structures yield new functions for light operation, thus improve significantly the imaging quality of optical systems [2]. Microgrooves can also be used as fluid channels in biomedical and biochemical applications. Therefore, high-precision and high-efficiency fabrication of microgrooves on flat or curved surfaces are receiving focused interests.

Commercially, glass and plastic are two major substrate materials for micro-structured components. Glass has predominant advantages over plastic on aspects of hardness, refractive index, light permeability, stability to environmental changes in terms of temperature and humidity, etc. A few microstructures on glass can be fabricated by material removal processes, such as sand blasting, photolithography, wet/dry etching, focused ion beam (FIB), and so on [3]. These processes are effective for manufacturing microstructures with rectangular cross sections (U-grooves), but difficult to fabricate microgrooves with sharp-angled cross sections (V-grooves). Microcutting of glass using microendmills has also been reported, but the production efficiency is limited and the

production cost is considerably high for mass production [4]. As an alternative approach, glass molding press (GMP) is able to produce glass optical elements by replicating the shape of the mold to heated glass preforms without further machining process [5–7]. From the viewpoint of fabrication cost and process time, the GMP technique is undoubtedly a better approach to produce precision optical elements, such as aspherical lenses, Fresnel lenses, diffractive optical elements (DOEs), microprism arrays, microlens arrays and so on. In recent years, glass molding for microstructure, alternatively termed hot embossing or thermal imprinting, has also been reported [8,9].

In the molding/embossing/imprinting process, mold fabrication is an important issue. Super hard materials, such as silicon carbide (SiC) and tungsten carbide (WC), are preferable mold materials for pressing continuous surfaces like aspherical lenses [10]. However, they have not been commonly used for molding microstructures because it is very difficult to generate microstructures into these materials. In embossing/imprinting research, glassy carbon (GC) molds fabricated by focused ion beam (FIB) or dicing were used [8,9]. Normally, the FIB technique is used to generate nanometer level microstructures on a small-area GC mold, and the dicing technique is used for fabricating 10 μm order or bigger microstructures on a large-area mold. In a previous study, the present authors demonstrated that electroless-plated nickel phosphorus (Ni–P) is a potential mold material for glass molding with a practically long mold life [11]. As Ni–P has excellent machinability in precision microcutting [12], GMP using Ni–P plated mold might be an effective way to generate 1–10 μm level microstructures on large-area

* Corresponding author. Tel.: +81 22 7956946; fax: +81 22 7957027.

E-mail address: yanjw@pm.mech.tohoku.ac.jp (J. Yan).

glass components, as preliminary demonstrated in a previous work [13].

The quality and production cost of the molded glass elements are strongly dependent on the shape transferability in GMP [14]. The shape transferability includes two aspects. One is the microscope shape transferring accuracy, which is defined by the form error between the molded glass element and the mold. The other is the stability of the thermo-mechanical properties of the mold, which is defined by the deformation of the mold before and after GMP. However, for the GMP of microstructures using Ni–P molds, both of the two aspects are still unclear.

Compared to experiments, finite element method (FEM) simulation is a relatively economical way to illustrate the details of the GMP process. In our previous work, the heat transfer phenomenon in GMP [15] and the thermo-mechanical constitutive equation of glass at high temperature [16] were modeled and simulated by FEM, respectively. In this paper, FEM simulation was carried out to study the characteristics of GMP for microgrooves under various conditions. Based on the simulation results, optimal molding conditions were determined, and GMP experiments were carried out. The shape of the formed microgrooves on the glass plate were measured and compared with that of the Ni–P mold. The change in shape and surface roughness of the mold was evaluated.

2. Glass molding press simulation

2.1. Modeling

In GMP, a glass preform is pressed at a temperature tens of degrees centigrade above its transition temperature to replicate the shape of the mold into the glass surface. At the molding temperature, glass shows high viscoelasticity. Viscoelasticity is a time-dependent response of a material to stress or strain. At a constant load, the glass strain is made up of instantaneous strain (elastic effect) and a continual strain as a function of time (viscous effect). This time-dependent deformation under a constant load is termed creep. On the other hand, when a constant strain is applied, the stress relaxes with the increase of time, which is termed stress relaxation. Creep and stress relaxation are the two main characteristics of glass deformation behavior during pressing and annealing in GMP.

Viscoelastic constitutive models are necessary to analyze the time-dependent creep behavior and stress relaxation of glass at high temperature. The simple Maxwell model, the Kelvin model, the Burgers model and the generalized Maxwell model are 4 typical constitutive models [17], which allow the rate of change of the inelastic strain to be a function of the total stress and previous strain. These models can be expressed by a series of springs and dashpots. The simple Maxwell model can fit stress relaxation, but is not suitable for modeling creep. The Kelvin model is unable to describe the time-dependent change of stress during creep. The Burgers model can simulate creep perfectly, as described in one of our previous paper [16]. It can be used to simulate stress relaxation too, but it was found that a deviation always happens at the beginning of the stress relaxation. Therefore, among the four kinds of models, the generalized Maxwell model might be the best one to describe creep and stress relaxation in the viscoelastic deformation of glass at high temperature.

In this work, a 5-pair generalized Maxwell model was set up to describe the glass deformation during the pressing stage, as schematically shown in Fig. 1. The time-dependent response is characterized by the deviatoric terms, as shown in Eq. (1):

$$\sigma(t) = \int_0^t G(t - \tau) \frac{d\varepsilon}{d\tau} d\tau \quad (1)$$

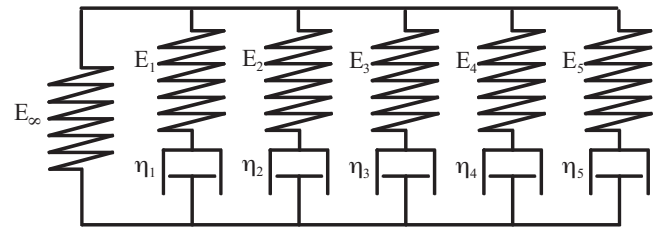


Fig. 1. The generalized Maxwell model for describing the viscoelasticity of glass.

The above integral is evaluated for current time t based on past time τ . $G(t - \tau)$ is not a constant value, but is represented by a Prony series as described by Eq. (2):

$$G(t) = G_0 \sum_{i=1}^n w_i e^{-t/t_{ri}} \quad (2)$$

where w_i is the relative moduli, t_{ri} is the reduced time, used to describe the shift in time due to temperature. The shift function ($A(T)$) used in this model is the Tool–Narayanaswamy (TN) shift function, as shown in Eq. (3):

$$\ln(A(T)) = \frac{H}{R} \left(\frac{1}{T_{ref}} - \frac{1}{T} \right) \quad (3)$$

where T_{ref} is the reference temperature. H is the activation energy, and R is the ideal gas constant.

The relative moduli w_i and the reduced time t_{ri} in Eq. (2) at the reference temperature T_{ref} (600 °C) are listed in Table 1, which were obtained by curve fitting in our previous research [16]. The infinite relaxation modulus w_∞ is 0.001. As the reduced time is very small due to the low viscosity at the molding temperature, viscous flow is the dominant mode of energy dissipation during pressing and annealing in GMP. Based on the generalized Maxwell model, the pressing and annealing stages of the GMP process were simulated under various conditions.

In this study, simulation of GMP was conducted using a commercial FEM code MSC.Marc, which is powerful in nonlinear solution for forging and molding process of various materials. The program is capable of simulating large deformation of material flow under isothermal or nonisothermal conditions. In the experiments of microgroove molding, there are 500 V-grooves on the mold spacing regularly in a 5 mm × 5 mm area. In the simulation, for simplification, only 8 grooves were calculated. Fig. 2 shows the two-dimensional simulation model of GMP for microgrooves. The upper mold is flat and fixed on the top; the lower mold with microgrooves will move upward to press the softened glass. The glass object was meshed by 48,000, 3-node, triangle, and plane strain solid elements. In order to guarantee the FEM simulation convergence in the glass-mold contact region and save remeshing time at the sharp corners during the simulation, the sharp ridges of the grooves on the top were rounded with a small radius of 1 μm on the top, while the sharp angle of the valley was kept as the actual size. The molds were modeled as rigid objects without deformation. As the glass preform is pressed at the same temperature as that of the molds, no heat transfer was considered in this simulation.

Table 1
Parameters of the generalized Maxwell model.

Term no.	Relative moduli w_i	Reduced time t_{ri} (s)
1	0.238	0.0070
2	0.238	0.0072
3	0.238	0.0075
4	0.238	0.0078
5	0.047	0.0010

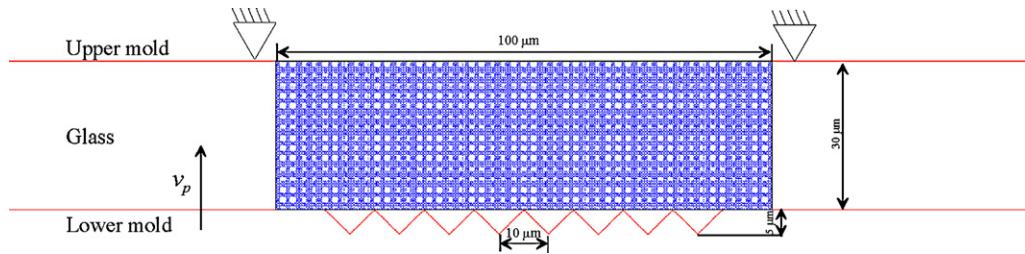


Fig. 2. Two-dimensional simulation model for GMP of microgrooves.

Table 2
Simulation parameters for various molding conditions.

Group no.	Molding temperature T_{mld} ($^{\circ}\text{C}$)	Pressing velocity v_p (mm/s)	Friction coefficient μ_f
1	560	0.1	0.1
	570		
	580		
	590		
2	570	0.01	0.1
		0.1	
		1	
3	570	0.1	0.1
			0.3
			0.5

2.2. Simulation results and discussion

FEM simulation was performed under 3 groups of conditions to illustrate the effects of molding temperature, pressing velocity and friction coefficient, respectively. The parameters of the simulation conditions are listed in Table 2.

First, the effects of molding temperature (T_{mld}) were studied at 560 $^{\circ}\text{C}$, 570 $^{\circ}\text{C}$, 580 $^{\circ}\text{C}$ and 590 $^{\circ}\text{C}$, respectively. The pressing velocity (v_p) was set to 0.1 mm/s, and the maximum upward displacement of the lower mold was set to 15 μm . The friction coefficient (μ_f) was specified to 0.1. In the simulation, the glass material flows from the center to the two sides. It fills the center groove of the mold first, and then fills the outer grooves later. When the displacement reaches 13.74 μm , the V-groove of the mold is completely replicated into the glass plate.

Fig. 3 shows the distribution of equivalent stress at a mold displacement of 15 μm at 570 $^{\circ}\text{C}$. The stress distribution is bilaterally symmetrical in the glass plate. The lowest stress occurs around the center groove and the highest stress takes place at the corners of the side grooves. As the molding temperature changed, the stress distribution pattern remained almost unchanged, but the highest and the lowest stresses changed greatly. Fig. 4 shows the changes in the maximum and the minimum equivalent stresses at different temperatures from 560 $^{\circ}\text{C}$ to 590 $^{\circ}\text{C}$. The lowest stress is more

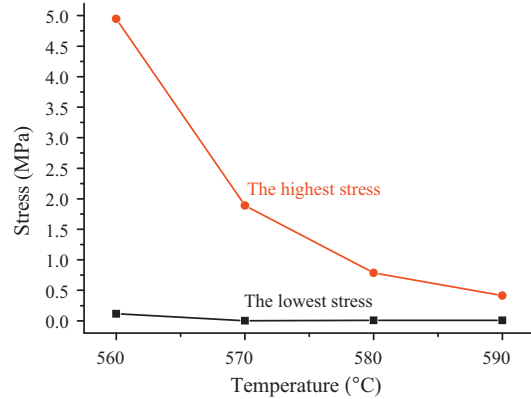


Fig. 4. Change of stress with molding temperature.

or less the same even at different temperatures, but the highest stress decreased to approximately 1/10 at 590 $^{\circ}\text{C}$ compared to that at 560 $^{\circ}\text{C}$.

Second, the effects of pressing velocity were investigated. The pressing velocity was set to three levels: 0.01 mm/s, 0.1 mm/s and 1 mm/s, respectively. The molding temperature was fixed at 570 $^{\circ}\text{C}$. The simulation results are shown in Fig. 5. The highest stress rises to 14.32 MPa at the pressing velocity of 1 mm/s, which is 7.6 times the highest stress at 0.1 mm/s, and 41 times that at 0.01 mm/s. These results agree well with the relationship in Eq. (1), i.e., the stress is proportional to the strain rate.

The selection of molding temperature and pressing velocity is based on three criteria: small mold deformation, long mold service life, and high productivity. Among the three criteria, the mold deformation is the first one to consider when fabricating precision optical components. As the high-temperature mechanical properties, such as yield strength and fatigue strength, of the Ni–P material are still unknown, we cannot yet determine exactly the critical stress which will cause mold deformation in the GMP process. In this paper, for simplicity, we take 2 MPa as the maximum

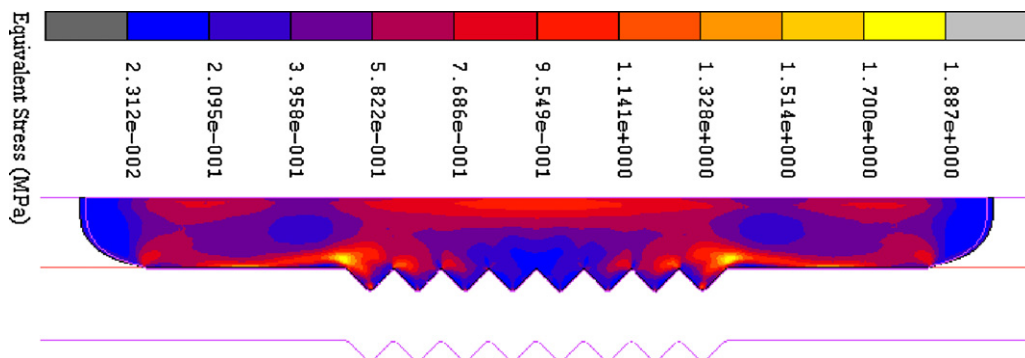


Fig. 3. Distribution of equivalent stress at a molding temperature of 570 $^{\circ}\text{C}$ ($T_{\text{mld}} = 570^{\circ}\text{C}$, $v_p = 0.1$ mm/s, $\mu_f = 0.1$).

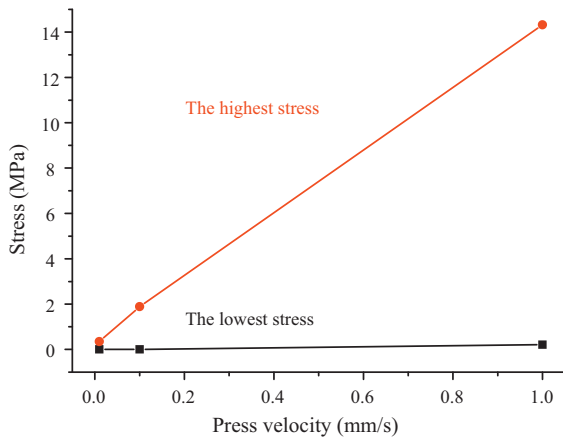


Fig. 5. Change of stress with pressing velocity.

stress, which is a pressure value usually used in glass embossing processes where GC and nickel cobalt (Ni–Co) were used as mold materials [9,18]. After the stress condition has been satisfied, the molding temperature should be as low as possible to prolong the mold life, and the pressing velocity should be as high as possible to improve production efficiency. As a result, the molding temperature of 570 °C and the pressing velocity of 0.1 mm/s were finally selected as the optimal pressing conditions for the later GMP experiments based on the results in Figs. 4 and 5.

Third, the effects of friction coefficient were investigated. The friction coefficient depends on the surface roughness of the molds, the release agent coating, and the glass preform, as well as the material affinity among these three. GMP simulation was performed by varying the friction coefficient from 0.1 to 0.5 at the glass–mold interfaces. A true stick-up friction model was adopted in the simulation. The molding temperature was 570 °C. Fig. 6 shows the change in stress at friction coefficients of 0.1, 0.3 and 0.5. The stress at friction coefficient 0.3 is higher than that at 0.1, but does not show noticeable change when the coefficient is further increased to 0.5.

Another interesting phenomenon observed in the simulation was that the higher the friction coefficient, the smaller the press displacement needed to form sharp V-grooves. For example, a displacement of 13.7 μm is needed at a friction coefficient of 0.1, but at friction coefficients of 0.3 and 0.5, the necessary displacements are only 10.8 μm and 10.1 μm. The reason for this phenomenon may be the difference in flow velocity of glass in the horizontal and vertical directions. At a high friction coefficient, glass is hard to flow in the horizontal direction. The increasing pressing load then eases the glass flow in the vertical direction. Consequently, glass is squeezed

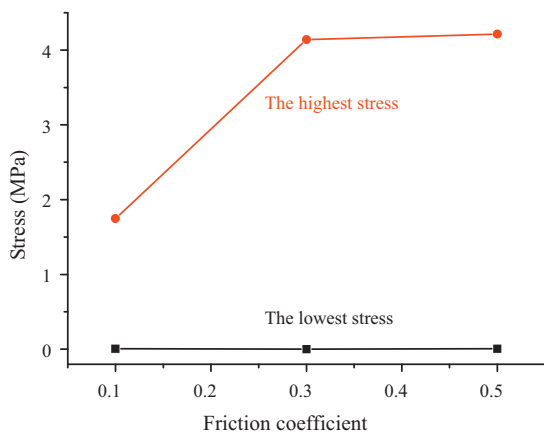


Fig. 6. Change of stress with friction coefficient.

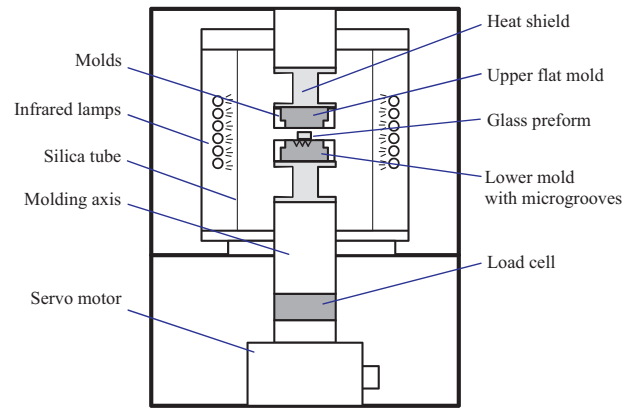


Fig. 7. Schematic diagram of the structure of the ultraprecision glass molding machine.

to fill up the V-grooves at a smaller press displacement. On the other hand, it should be noted that a high friction coefficient leads to a high stress at the glass–mold interface, which might cause mold deformation and deflection of the glass component. This issue must be comprehensively considered when molding extremely thin glass components.

3. Glass molding press experiments

3.1. GMP machine, mold and glass preform

The GMP experiments were performed using an ultraprecision glass molding machine, GMP211 (Toshiba Machine Co., Ltd., Shizuoka, Japan), the structure of which is schematically shown in Fig. 7. Nitrogen gas was used to purge the air to protect the molds from oxidation at high temperature. The molding chamber was covered with a transparent silica tube, which can let the infrared rays in while separating the nitrogen gas from the air outside. After the glass preform reached the molding temperature, the lower mold was driven upward to close the molds, while the upper mold was held stationary. In this way, the microstructures on the mold surface were replicated to the glass plate. Then, annealing was conducted to release the internal stress. Finally the molded glass plate was cooled to room temperature naturally.

The upper mold has a flat polished surface, and the lower mold, as shown in Fig. 8, has micro V-grooves on its surface. The lower mold is a cylindrical stainless steel blank with a diameter of 50 mm

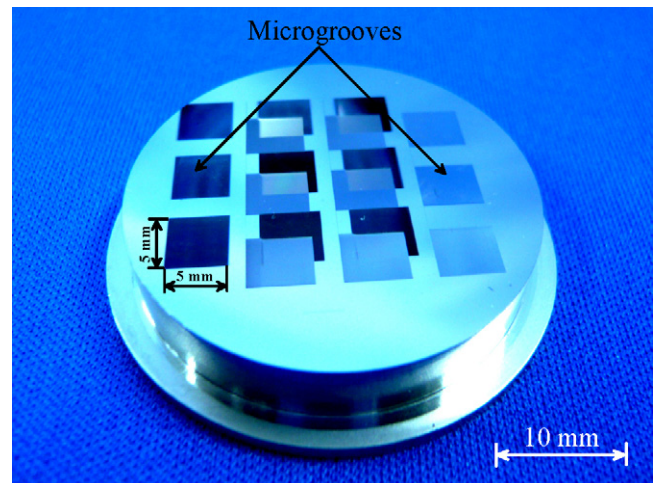


Fig. 8. Photograph of the Ni–P mold with microgrooves.

electroless-plated with Ni–P. The thickness of the Ni–P layer was approximately 100 μm . As the thermal expansion ratio of Ni–P ($11.5\text{--}14.5 \times 10^{-6} \text{ 1/}^\circ\text{C}$) is slightly different from that of stainless steel ($14.7\text{--}20.2 \times 10^{-6} \text{ 1/}^\circ\text{C}$), sometimes thermal bending of the mold takes place during temperature changes. In this work, a thick stainless steel blank (5 mm) was used to improve the rigidity of the mold. Micro diamond turning was performed to flatten the Ni–P plated surface before machining microgrooves. A sharply angled cutting tool made of single crystalline diamond was used for cutting microgrooves on the mold. By periodically shifting the tool in the cutting direction while the depth of cut is kept constant, parallel microgroove arrays were generated. The depth is 5 μm , and the pitch is 10 μm , and the cross section of microgroove is isosceles right triangle with a vertex angle of 90° , and its profile has been shown in the simulation model in Fig. 2. Normally, release agent coatings are spattered on the mold surface to prevent glass adhesion and glass–mold interface reaction [19]. In this work, to observe the mold deformation in only a few press shots, we did not sputter the release agent coating and used the micro-cut Ni–P plated mold directly for GMP.

A typical low T_g (glass transition temperature, 506°C) glass, L-BAL42, produced by Ohara Inc., Kanagawa, Japan, was selected as test pieces. The shape of the glass preform is approximately ellipsoidal, having a semimajor axis of 5.25 mm and a semiminor axis of 3.65 mm. The glass preform was freely placed on the lower mold before pressing without fixing. This situation is the same as that in the FEM simulation. The molding tests were performed in the nitrogen gas environment.

The glass pieces were pressed at the highest pressing load of 1000 N. Temperatures of the upper and lower molds are monitored by two thermocouples beneath the surfaces of the two molds with a measurement accuracy of $\pm 1^\circ\text{C}$. The position of the lower mold is recorded by the encoder with a resolution of 0.1 μm . A load cell is placed beneath the lower axis as a feedback of the pressing load with a resolution of 0.98 N. From the simulation results in Section 2, an intermediate molding temperature of 570°C , and a slow pressing velocity of 0.1 mm/s were selected as the optimal pressing conditions in the GMP experiments.

After the GMP experiments, the pressed glass piece was released from the mold using a vacuum sucking device. The form accuracy of the mold and molded microgrooves were then measured by a three-dimensional laser scanning microscope, Keyence, VK-8500, which has a resolution of 0.001 μm . The magnification of the objective lens used is 100 times and the total magnification is 2000 times. The monochrome light auto run mode was used in the measurement.

3.2. Experimental results and discussion

Fig. 9 is a photograph of a glass plate with molded microgrooves. At a view angle smaller than the critical angle of reflection, colors can be seen on the part of the microgrooves. This is a result of the optical characteristics of the microgrooves. The path of the light being reflected is changed by the regularly spaced microgrooves, leaving a colorful relief pattern on it.

Fig. 10 shows a micrograph of the microgrooves on the mold before the molding process. Fig. 11 shows a micrograph of the molded microgrooves on the glass plate. Clear parallel microgrooves have been replicated into the glass surface. Next, the two-dimensional sectional profiles of the molded glass plates and the grooved mold were measured. As shown in Fig. 12, the depth of the microgrooves of the mold is $4.85 \pm 0.038 \mu\text{m}$, while that of the microgrooves of the molded glass plate is $4.71 \pm 0.010 \mu\text{m}$. Therefore, the transfer accuracy, defined by the form error between the Ni–P mold and the molded glass plate, is approximately 0.14 μm .

Although the cross-sectional profile and the depth of the microgrooves could be measured by the laser scanning microscope,

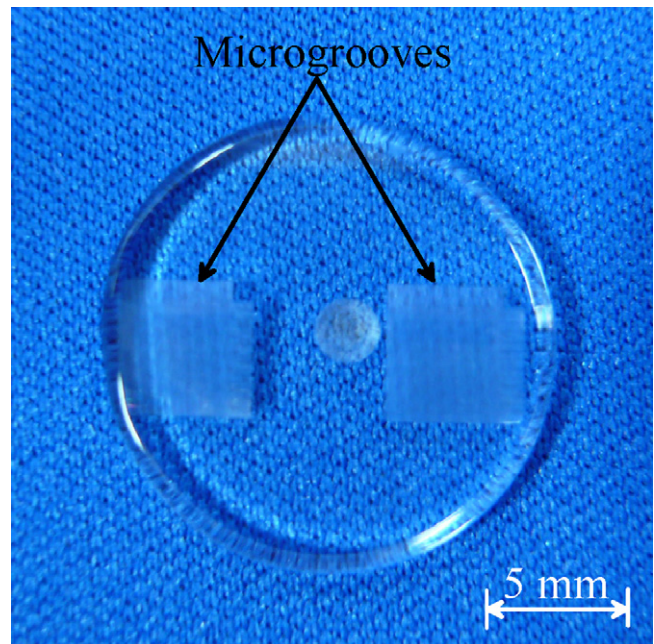


Fig. 9. Photograph of a glass plate with molded microgrooves.

the profiling results at the ridges and valleys of the grooves might not be accurate. As the laser beam used for measurement has a diameter of 1 μm , which is comparable to or larger than the corner radius of the groove ridge and valley, a big change of incident angle at the ridges and valleys of the groove might cause measurement errors. In order to confirm the corner radius of the microgrooves precisely, one of the molded glass pieces was cut at the direction perpendicular to the V-grooves by a diamond saw, and then, the cross-sectional surface was finely polished. The micrograph of the cross-sectional surface of the grooves is shown in Fig. 13. It is seen that the replicated V-grooves have a sharp angle of 90° at the ridges. Therefore, we can deduce that the glass material has completely filled up the V-grooves on the Ni–P mold during GMP. However, it is

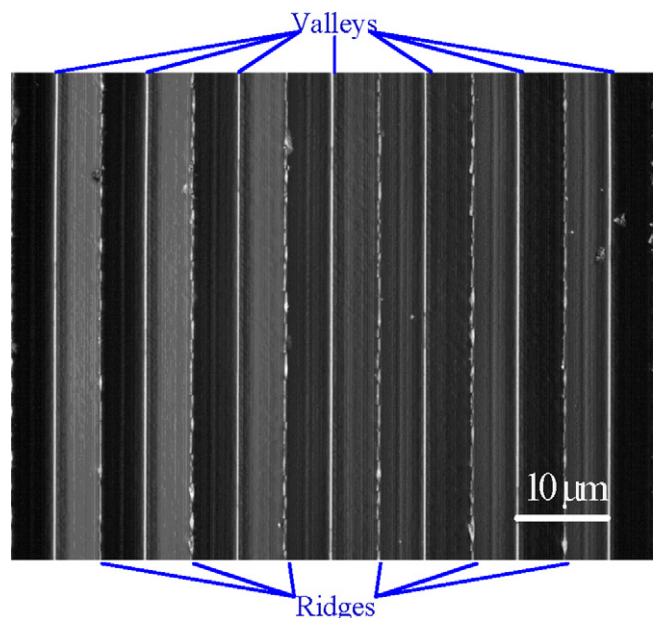


Fig. 10. Micrograph of the microgrooves on the Ni–P mold before GMP.

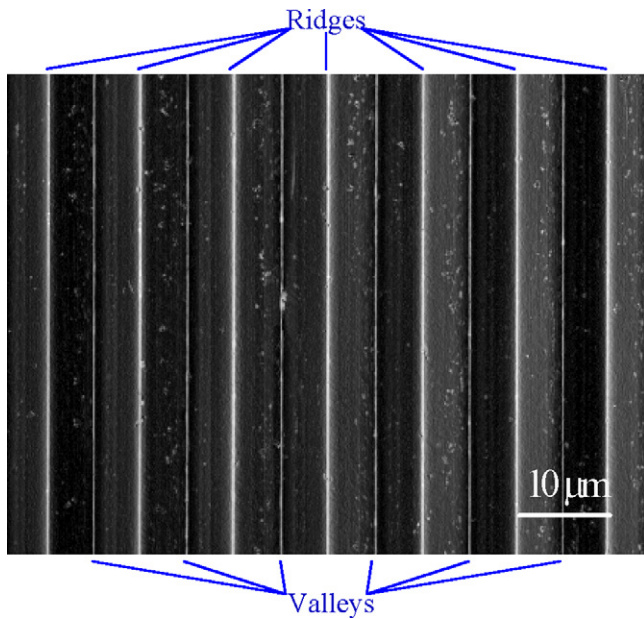


Fig. 11. Micrograph of the molded microgrooves on the glass plate.

noted that the valleys of the V-grooves on the glass plate are slightly rounded, having a corner radius of about 0.5 μm. The reason for this phenomenon might be due to the microscopic deformation of the Ni–P mold taking place at the sharp ridges of the microgrooves.

In addition, repetitive GMP experiments showed that as the shot number increased, the shape and the surface roughness of the microgrooves on the Ni–P mold changed gradually, which led to profile distortion of the molded microgrooves on glass. For example, Fig. 14(a) and (b) are scanning electron microscope (SEM) micrographs of the microgrooves on the Ni–P mold before the GMP experiments and that after 25 press shots, respectively. The groove valleys remained almost unchanged, but the groove ridges were slightly distorted and rounded. Also, small bulges can be seen on the surface of the mold.

From the SEM photographs, we can estimate that the shape change of the microgroove on the mold is from a few tens of nanometers to one hundred and a few tens of nanometers. This shape error is in the same level as the form error between the mold and the molded glass plate, namely, 140 nm (0.14 μm), as shown in

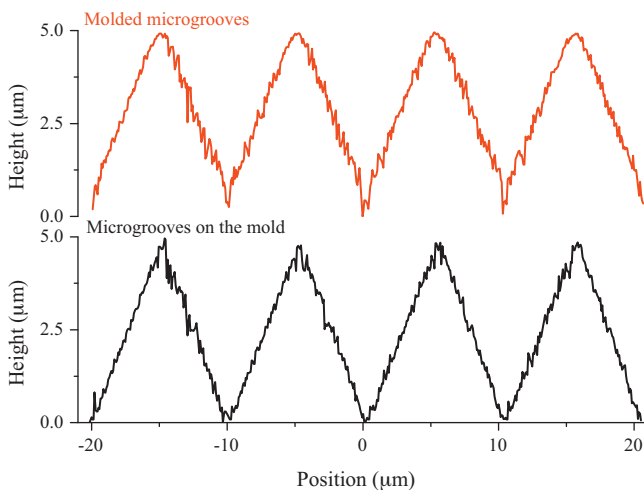


Fig. 12. Comparison of cross-sectional profiles of the microgrooves on the mold and those on the molded glass plate.

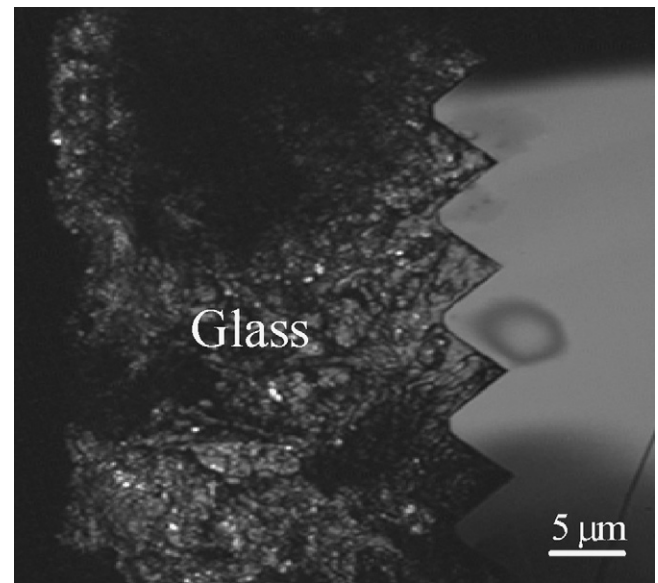


Fig. 13. Cross section micrograph of the molded microgrooves on a glass plate.

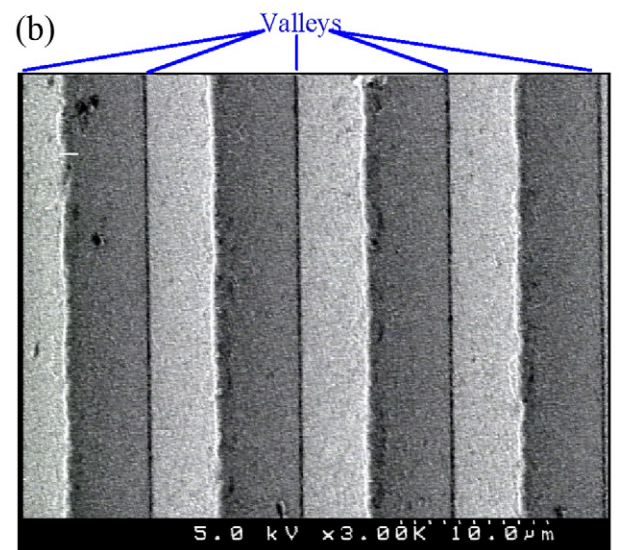
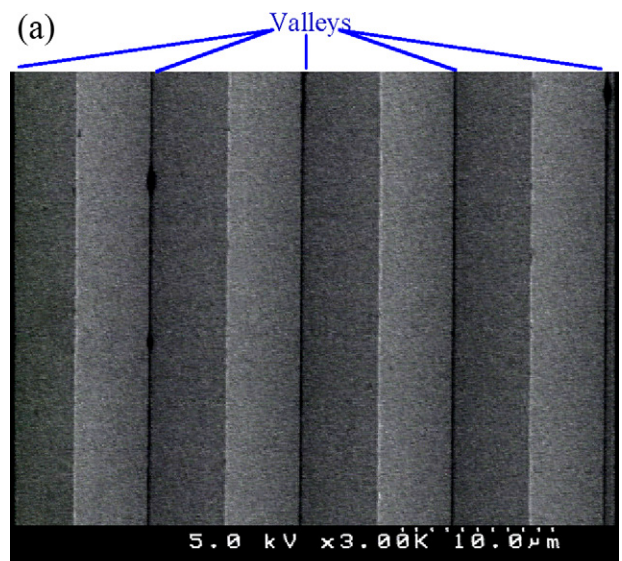


Fig. 14. SEM micrographs of microgrooves on the mold: (a) before GMP and (b) after GMP.

Fig. 12. Therefore, it is presumable that the form error in the GMP of microgrooves is mainly due to the gradual plastic deformation at the groove ridges of the mold. In Fig. 14, we can also see clearly that the mold surface has been roughened, although it was difficult for us to precisely measure the change in surface roughness of the angled groove surface by available measurement equipment. The surface roughening phenomenon might be due to the atomic diffusion between the mold and the glass material, as has been discussed in one of our previous papers [19]. It is a future task to explore inactive release agent coatings and improve the high temperature strength of the Ni–P mold to prolong the service life of the mold in high-temperature GMP.

4. Conclusions

The GMP process of microgrooves has been investigated by both FEM simulation and experiments. The following conclusions are obtained.

1. The lowest stress occurs around the center of glass and the highest stress takes place at the corners of the side grooves. The highest stress decreases significantly as the molding temperature increases, and increase proportionally to the press velocity.
2. The stress in glass increases with the friction coefficient at the mold–glass interface, but remains constant when the friction coefficient is further increased from 0.3. The higher the friction coefficient, the smaller the press displacement needed for complete replication of grooves.
3. Extremely sharp ridges can be formed on glass, but the groove valleys become slightly rounded (corner radius $\sim 0.5 \mu\text{m}$). The replication accuracy from the Ni–P plated mold to the glass plate is approximately $0.14 \mu\text{m}$. The form error is mainly due to the deformation of the Ni–P mold at the sharp ridges.

Acknowledgements

This work has been supported by Japan Society for the Promotion of Science, Grant-in-Aid for Scientific Research (B), project numbers 19360055 and 203234. The authors would also like to thank Toshiba Machine Corporation for the technical supports during the experiments. Thanks are also extended to Ohara Corporation for providing glass samples and technical data.

References

- [1] Evans C, Bryan J. “Structured”, “textured” or “engineered” surfaces. CIRP Annual 1999;48:541–56.
- [2] Yan J. Ultraprecision machining for Fresnel lenses and their molds. In: Design and manufacturing of rear-projection optical systems. Tokyo: Technical Information Institute; 2006. p. 73–94 [chapter 3].
- [3] Chao CH, Shen SC, Wu JR. Fabrication of 3-D submicron glass structures by FIB. Journal of Materials Engineering and Performance 2009;18:878–85.
- [4] Matsumura T, Hiramatsu T, Shirakashi T, Muramatsu T. A study on cutting force in the milling process of glass. Journal of Manufacturing Processes 2005;7(2):102–8.
- [5] Yi A, Jain A. Compression molding of aspherical glass lenses – a combined experimental and numerical analysis. Journal of the American Ceramic Society 2005;88:579–86.
- [6] Katsuki M. Transferability of glass lens molding. In: Proceedings of SPIE, 2nd international symposium on advanced optical manufacturing and testing technologies. 2006. p. 61490M.
- [7] Klocke F, Dambon O, Sarikaya H, Pongs G. Investigations to the molding accuracy of complex shaped glass components. In: Proceedings of the euspen international conference. 2008.
- [8] Takahashi M, Sugimoto K, Maeda R. Nanoimprint of glass materials with glassy carbon molds fabricated by focused-ion-beam etching. Japanese Journal of Applied Physics 2005;44(7B):5600.
- [9] Takahashi M, Murakoshi Y, Maeda R, Hasegawa K. Large area microhot embossing of pyrex glass with GC mold machined by dicing. Microsystem Technologies 2007;13(3):379–84.
- [10] Yan J, Zhang Z, Kuriyagawa T. Mechanism for material removal in diamond turning of reaction-bonded silicon carbide. International Journal of Machine Tools and Manufacture 2009;49(5):366–74.
- [11] Masuda J, Yan J, Kuriyagawa T. Application of the NiP-plated steel molds to glass lens molding. In: 10th international symposium advances in abrasive technology. 2007. p. 123–30.
- [12] Yan J, Sasaki T, Tamaki J, Kubo A, Sugino T. Chip formation behavior in ultraprecision cutting of electroless nickel plated mold substrates. Key Engineering Materials 2004;3(8):257–8.
- [13] Yan J, Oowada T, Zhou T, Kuriyagawa T. Precision machining of microstructures on electroless-plated NiP surface for molding glass components. Journal of Materials Processing Technology 2009;209(10):4802–8.
- [14] Yan J, Zhou T, Yoshihara N, Kuriyagawa T. Shape transferability and microscopic deformation of molding dies in aspherical glass lens molding press. Journal of Manufacturing Technology Research 2009;1(1–2):85–102.
- [15] Yan J, Zhou T, Masuda J, Kuriyagawa T. Modeling high-temperature glass molding process by coupling heat transfer and viscous deformation analysis. Precision Engineering 2009;33(2):150–9.
- [16] Zhou T, Yan J, Masuda J, Kuriyagawa T. Investigation on the viscoelasticity of optical glass in ultraprecision lens molding process. Journal of Materials Processing Technology 2009;209(9):4484–9.
- [17] Pipkin AC. Lectures on viscoelasticity theory. New York: Springer-Verlag; 1972.
- [18] Pan CT, Wu TT, Chen MF, Chang YC, Lee CJ, Huang JC. Hot embossing of micro-lens array on bulk metallic glass. Sensors and Actuators A: Physical 2008;141(2):422–31.
- [19] Masuda J, Yan J, Tashiro T, Fukase Y, Zhou T, Kuriyagawa T. Microstructural and topographical changes of Ni–P plated molds in glass lens pressing. International Journal of Surface Science and Engineering 2009;3(1–2):86–102.